Global J. Environ. Sci. Manage. 11(3): 1035-1056, Summer 2025, Serial #43

Global Journal of Environmental Science and Management
(GJESM)

Homepage: https://www.gjesm.net/

Podcasts

ORIGINAL RESEARCH PAPER

Removal of cadmium and lead using a sub-bituminous coal resin modified with xanthate groups

F. Fuentes-Gandara[1,*], W. Cabrera-Lafaurie[2], I. Piñeres-Ariza[3], E. Espinosa-Fuentes[4], J. Marrugo-Negrete[5], J. Pinedo-Hernández[5]

[1] *Department of Natural and Exact Sciences, Universidad de la Costa, Calle 58 Nº 55-66, Barranquilla, Colombia*

[2] *Corporación Universitaria de Ciencias Empresariales, Educación y Salud – Corsalud, Calle 64 N° 52-62, Barranquilla, Colombia*

[3] *Department of Physics, Faculty of Basic Sciences, Universidad del Atlántico, km 7 Antigua vía Puerto Colombia, Colombia*

[4] *Faculty of Engineering, Universidad Libre, Cra 51B #135 -100, Cra 46 N° 48-170, Barranquilla, Colombia*

[5] *Faculty of Basic Sciences, Department of Chemistry, Universidad de Córdoba, Cra 6 #77-305, Montería, Colombia*

ARTICLE INFO

Article History:
Received 16 February 2025
Revised 21 April 2025
Accepted 23 May 2025

Keywords:
Coal
Heavy metal
Isotherms
Removal
Wastewater

DOI: 10.22034/gjesm.2025.03.10

ABSTRACT

BACKGROUND AND OBJECTIVES: The increase in industrial effluent discharges from sectors such as smelting, electroplating, pharmaceuticals, and ceramics has led to a rise in heavy metal presence in ecosystems, posing a growing environmental risk. As the demand for more efficient materials rises, there has been a heightened interest in employing adsorbents obtained from biological origins and industrial waste, owing to their affordability, accessibility, and efficacy in eliminating heavy metals from aqueous environments. The objective of this study was to assess the potential of a modified adsorbent resin, synthesized from mineral coal waste originating in Cesar, Colombia, for the removal of cadmium and lead from aqueous solutions as a sustainable remediation strategy.

METHODS: The coal waste was chemically modified using sodium hydroxide and carbon disulfide to synthesize the adsorbent resin. Batch adsorption experiments were performed at hydrogen ion concentration levels from 3 to 8 to analyze the removal efficiency. The effect of hydrogen ion concentration on adsorption efficiency was examined, and the experimental results were analyzed using a comparative modeling technique. Adsorption equilibrium was assessed using the Freundlich, Langmuir, and Langmuir–Freundlich isotherms, while kinetic behavior was interpreted through pseudo-first- and second-order models.

FINDINGS: The results demonstrated that the removal efficiencies varied with potential of hydrogen, reaching maximum values when it was adjusted to 6, with 98 percent for lead and 97 percent for cadmium. The adsorption process conformed to the Freundlich isotherm, implying a multilayer adsorption mechanism, and the pseudo-second-order kinetics revealed that chemisorption was the prevailing mechanism.

CONCLUSION: The findings of this study underscored the effectiveness of modified mineral coal waste as a viable adsorbent for the extraction of cadmium and lead, suggesting a promising option for the treatment of industrial wastewater. Besides its exceptional performance, this strategy contributes to the valorization of solid waste from coal mining, encouraging a circular economy and minimizing the environmental impact associated with its disposal.

This is an open access article under the CC BY license (http://creativecommons.org/licenses/by/4.0/).

NUMBER OF REFERENCES	NUMBER OF FIGURES	NUMBER OF TABLES
90	7	3

*Corresponding Author:
Email: *fabioar20@hotmail.com*
Phone: +300 5616 226
ORCID: 0000-0002-0681-0544

Note: Discussion period for this manuscript open until Sep 1, 2025 on GJESM website at the "Show Article".

INTRODUCTION

Industrial development and population growth in countries at various stages of development have exacerbated environmental concerns, including wastewater contamination with heavy metals, which poses global threats to biodiversity and human health (Ben-Ali *et al.,* 2017; Wattanakornsiri *et al.,* 2022). The introduction of heavy metals into aquatic ecosystems arises from a range of industrial activities, including mining, pesticide and battery manufacturing, electroplating, leather tanning, metal plating, steel metallurgy, pigment and dye synthesis, petroleum product production, as well as paper and textiles, and the discharge of leachate from landfills (Tambaru *et al.,* 2018; Tamizharasan *et al.,* 2023; Sulistyowati *et al.,* 2023). The presence of heavy metal elements in water resources is quite alarming, especially considering the harmful effects of these contaminants, their extensive distribution, environmental durability, and their ability to bioaccumulate in living organisms and biomagnification across trophic levels (Fuentes-Gandara *et al.,* 2021). Heavy metals are recognized as one of the major environmental issues and are considered among the most dangerous contaminants due to rigorous regulatory standards (Sabilillah *et al.,* 2023). Therefore, it is essential to eliminate them from wastewater and industrial discharges to safeguard both public health and the ecosystem (Jasim and Ajjam, 2024). In biological entities, exposure to heavy metals may result in numerous disorders and diseases, including complications in respiration, dysfunction of the endocrine system, obesity, developmental abnormalities in fetuses, neurological issues, infertility, miscarriages, multiple cancer types, and even fatal outcome (Mitra *et al.,* 2022; El Mouden *et al.,* 2023). In many regions of the world, lead (Pb) and cadmium (Cd) are identified as high-priority inorganic environmental pollutants (Akinterinwa *et al.,* 2022; Arul *et al.,* 2023). Annual global emissions of Cd and Pb from human activities are estimated at approximately 3000 and 120000 tons, respectively. Specifically, divalent cations Cd and Pb pose considerable threats when present in water bodies (Wang *et al.,* 2024a). Pb exposure can cause adverse effects on the human body, including mental retardation, impairment of the nervous and reproductive systems, anemia, damage to red blood cells and kidneys, hypertension, and cardiovascular problems. Severe lead exposure may result in infertility, miscarriages, and neonatal death (Arul *et al.,* 2023). Acute and chronic disorders associated with cadmium exposure include kidney damage, hypertension, emphysema, potential direct inhibition of deoxyribonucleic acid (DNA) mismatch repair, itai-itai disease, testicular atrophy, and certain types of cancer (Požgajová *et al.,* 2022). In light of the toxic risks posed by heavy metals, the advancement of research dedicated to the removal of these contaminants from wastewater is gaining significant importance (Karim *et al*., 2019; Li *et al*., 2021; Cheng *et al*., 2022) to ensure the protection of human health and the environment against the adverse effects of Cd and Pb contamination (Arul *et al.,* 2023). Various techniques are available for removing heavy metals from aqueous wastewater solutions, such as reverse osmosis, ultrafiltration, ion exchange, electrodeposition, chemical precipitation, and membrane filtration. Despite their advantages, these techniques present multiple drawbacks, including the creation of substantial waste, elevated operational costs, limited selectivity, and insufficient removal effectiveness (Khan *et al.,* 2020; Fakhar *et al.,* 2021). Among the diverse methods available for treating contaminated water, adsorption stands out as an effective and practical approach for removing heavy metals. Its advantages include operational simplicity, cost-efficiency, and high removal performance, positioning it as a favored option in physicochemical treatment strategies. Adsorption techniques are particularly appealing due to their adaptability for wastewater treatment (Gebretsadik *et al.,* 2020; Chakraborty *et al.,* 2022), often relying on adsorbents made from naturally abundant materials or byproducts from agricultural and industrial processes. Low-cost adsorbents are characterized by minimal processing requirements and accessibility, whether derived from natural sources or as industrial residues. Another major hurdle in this domain is the advancement of adsorbents that possess improved adsorption rates, selectivity, recyclability, and capacity, catering to the rising demand for efficient and eco-friendly solutions to heavy metal contamination (Jawad *et al.,* 2020). Studies have been carried out to explore methods for removing and recovering toxic metals using resins with unique functional characteristics (Gurnule and Katkamwar, 2012). Ion exchange materials, including zeolite and Purolite C105, have demonstrated exceptional

performance in extracting heavy metal ions from aqueous solutions. Zeolite achieved removal efficiencies of 98 percent (%) for copper (Cu), 93% for nickel (Ni), and 88% for Pb, while Purolite C105 showed removal rates of 94%, 97%, and 88% for the same metals, respectively (Mohammed *et al.,* 2013). The cationic resin Purolite® C100, applied in an acidic medium, was used for the remediation of Pb and Cu contamination. Ion exchange achieved removal efficiencies of 92.9% for Pb and 94.37% for Cu. These findings were derived from a dosage of Purolite® C100 resin that varied from 40 gram (g) to 80 g, within a potential of hydrogen (pH) range of 3 to 12 (Jasim and Ajjam, 2024). Selective ion exchange resins have been widely used for the removal of other heavy metals in aqueous solutions, such as chromium (Cr) (Gode and Pehlivan, 2003), Cd (Memon *et al.,* 2007; Wong *et al.,* 2014), aluminum (Al) and iron (Fe) using the aminomethylphosphonic acid functional chelating resin (Virolainen *et al.,* 2021). Coal fly ash, produced from coal-burning power plants, is acknowledged for its dusty waste nature, loose structure, and consistent pore distribution, rendering it a highly porous material with multiple uses (Patel, 2020). Its use as an adsorbent is particularly valued due to its accessibility, high efficiency in treatment processes, and cost-effectiveness (Sun *et al.,* 2022). When enhanced with sulfonated materials using alkaline fusion and hydrothermal processes, coal fly ash has shown to be effective in the simultaneous removal of Cd and methylene blue dye from wastewater. Under optimized conditions, adsorption capacities reached 93.53 milligrams per gram (mg/g) for Cd and 116.69 mg/g for methylene blue in single systems, and 85.49 mg/g for Cd and 100.23 mg/g for methylene blue in binary systems (Wang *et al.,* 2024b). The modification of fly ash through a low-temperature fusion method using potassium hydroxide (KOH) as an activator has significantly enhanced its adsorption capacity for the removal of heavy metals from aqueous solutions. This material proves to be highly effective in the removal of Pb, Cd, and Cu from wastewater. Under optimal conditions, the maximum adsorption capacities were reported as 337.41, 310.09, and 125 mg/g, respectively, in single-metal systems (Yang *et al.,* 2023). Fly ash modified with zeolites is classified as a high-efficiency adsorbent. In a batch process under optimal conditions, this material demonstrated great potential for metal removal, achieving removal efficiencies of 99.04% for Cu and 97.73% for Ni (Sireesha *et al.,* 2022). Lignite, recognized as the most immature form of coal, exists between peat and bituminous coal in the carbonization spectrum. Its defining features include a dark brown color and elevated reactivity. This material contains various functional groups such as phenolic hydroxyl, hydroxyl, aldehyde, carboxyl, and carbonyl. Additionally, lignite exhibits significant properties, including a notable capacity for cation exchange, a large surface area, and outstanding chemical and biological durability (Yuliani *et al.,* 2012). These features empower it to efficiently reduce the movement and environmental accessibility of heavy metals in soils and industrial discharges (Kamaraj *et al.,* 2025). Modifications with nanoferric iron have been recognized as a straightforward, efficient, and economical strategy, garnering substantial attention in scientific research. As an illustration, doping lignite with nanoferric iron has been proven to increase its ability to adsorb Cd by 36% (Pentari *et al.,* 2019). Furthermore, acidic treatments of lignite have been employed to further improve its capacity for removing metal ions from wastewater. After treatment with nitric acid (HNO_3), the adsorption of Pb ions by modified lignite was predominantly achieved through chemical adsorption involving mainly ion exchange, coordination, and chelation between the metal ions and the adsorbent (Wang *et al.,* 2021). A noteworthy material for environmental applications, particularly in addressing heavy metal contamination, is mercapto-modified coal gangue. Studies have demonstrated that incorporation of mercapto groups successfully generates functional sites that improve the adsorption of heavy metal ions, including mercury (Hg), Cd and Pb. This modification enables the material to achieve adsorption capacities of 110.4, 179.2 and 332.8 mg/g, for these metals, respectively (Shang *et al.,* 2021). Finally, considering that mineral coal waste is a low-cost material with limited economic reuse in many sectors, its disposal has caused significant degradation of natural resources and poses environmental risks. However, these residues exhibit resistance to high temperatures, dimensional stability, and high viscosity, allowing them to be used in the production of resins for metal ion exchange applications. In this context, the goal of this study is to analyze the capability of a chemically altered resin obtained from mineral coal waste for the extraction of Cd and Pb

from aqueous solutions, employing adsorption experiments backed by kinetic and isotherm modelling. The experimental development of this research was conducted in the laboratories of the Department of Natural and Exact Sciences at Universidad de la Costa and the Faculty of Basic Sciences at Universidad de Córdoba, in Colombia in 2023.

MATERIALS AND METHODS

The methodology involved the preparation of an adsorbent from sub-bituminous coal, which was chemically modified and characterized through compositional analyses (proximate and ultimate), alongside the application of fourier transform infrared spectroscopy (FTIR). Both unmodified (C) and modified (CM) coal samples were evaluated for the removal of Pb and Cd ions from aqueous solutions using batch adsorption experiments conducted under varying pH conditions. These tests encompassed equilibrium and kinetic studies that were aligned with mathematical models illustrating processes which seem to adhere to follow first or second order kinetics. In this study, analytical-grade chemical compounds were used, supplied by Merck. These compounds include sodium hydroxide (NaOH), lead nitrate ($Pb(NO_3)_2$, carbon disulfide (CS_2), hydrochloric acid (HCl) and tetrahydrated cadmium nitrate ($Cd(NO_3)_2$ *$4H_2O$).

Collection and characterization of coal

A sub-bituminous coal from a mine located in the Cesar Department-Colombia was selected, an area known for its high coal production, accounting for 53.1% of the national production in 2022 with 30.2 million tons (United Nations Development Programme-UNDP, 2024). This coal is sourced through open-pit mining, facilitating the simultaneous collection of different strata, thus ensuring consistency in its attributes. This coal exhibits favorable thermal characteristics, low sulfur and ash content, and low nitrogen oxide emissions. The surface area of the resin was determined using the Brunauer, Emmett, and Teller (BET) method with a Micromeritics Gemini III 2375 sorptometer. Nitrogen adsorption-desorption isotherms were analyzed to calculate the specific surface area (Benkő *et al.,* 2013). Standard tests to determine the volatile matter, moisture, and ash content of the coal were carried out in accordance with the American Society for Testing Materials (ASTM) standards, specifically ASTM D 5832, 2867, and 2866, respectively (Pereira *et al.,* 2018). The characterization process for the adsorbents was carried out by obtaining the infrared spectra of C and CM by mixing and macerating 1 milligram (mg) of the sample with 100 mg of potassium bromide (KBr). The mixture was compressed to form a pellet, which was analyzed with using FTIR with Shimadzu 8400 device in the range of 4000 to 400 per centimeter (/cm) to determine the functional groups involved in the adsorption of heavy metals. The identification of potential xanthate traces in the aqueous medium was conducted using ultraviolet visible (UV-Vis) spectroscopy with a spectrophotometer functioning within the 200–800 nanometer (nm) range. A calibration curve was prepared using standard solutions at concentrations of 0.2, 1.0, 2.5, 5.0, and 10.0 parts per million (ppm), measuring their absorbance within the characteristic xanthate ion range of 230–300 nm. For the leaching analysis, 10 milliliters (mL) of the supernatants were collected after suspending 0.5 g of functionalized carbon in 50 mL of distilled water were collected. These suspensions were stirred at room temperature for 24, 48, 72, 96, and 120 hour (h). The samples were then filtered using 0.45 micrometer (µm) membranes and analysed with the spectrophotometer (Fontenele *et al.,* 2007).

Resin preparation

Initially, the collected coal was immersed in an acetone solution for a duration of seven days to promote its expansion. It was then repeatedly rinsed with distilled water until the conductivity of the rinse water stabilized, followed by a drying period of 24 h. The obtained material was ground in a mill to reduce the particle size and then sieved to achieve a particle size of 0.225 millimeter (mm). To eliminate certain dyes and impurities, the material underwent rinsing with 0.1 molarity (M) HCl followed by rinsing with distilled water until a neutral pH was reached. Subsequently, 25 g of the obtained material were placed in a beaker, to which 0.42 liters (L) of a NaOH (4M) solution was added and mechanically stirred for 3 h. Then, 102 mL of pure CS_2 was added, and the mixture was stirred for 3.5 h. Subsequently, the mixture was allowed to rest for 16 h, filtered, continuously rinsed with deionized water, and dried

at 70 degrees Celsius (°C) (Liang *et al.,* 2010). The resulting product was referred to as CM.

Adsorption tests

The impact of pH on Pb and Cd adsorption was evaluated by combining 50 mg of CM and C with 10 mL of a 100 ppm solution of each metal separately at 25°C. The experiments were conducted over a pH range of 3 to 8, adjusted using 0.1 M HCl and 0.1 M NaOH. After 8 h of stirring, the solutions were filtered, and the concentrations were assessed via an inductively coupled plasma optical emission spectrometer (ICP-OES).

For the kinetic study of Pb and Cd, 50 mg of adsorbent (CM) were mixed with 10 mL of $Pb(NO_3)_2$ and $Cd(NO_3)_2{\cdot}4H_2O$ solution, at a concentration of 100 ppm of Pb^{2+} and Cd, at an optimal pH value of 6. Samples were filtered and concentration measurements were documented at 60-minutes (min) intervals over a total duration of 8 h (covering the range of 60-480 min). The quantity of adsorbed metal was computed, using eq. 1 (Kumar *et al.,* 2023):

$$[q_e]=\frac{(C_o-C_e)\times V}{W} \quad (1)$$

Where; C_0 (mg/L) indicates the initial concentration, C_e (mg/L) represents the equilibrium concentration, q_e (mg/g) the equilibrium adsorption capacity, V (L) Volume of solution and W (g) is the adsorbent mass.

For the isotherm study, solutions with different concentrations of $Pb(NO_3)_2$ and $Cd(NO_3)_2{\cdot}4H_2O$ (1 - 45 ppm) were prepared using CM and C for 8 h. The amount adsorbed of both metals was determined with an ICP-OES.

All adsorption equilibrium isotherm data were evaluated according to the Freundlich, Langmuir, and Langmuir-Freundlich isotherm models, using Eqs. 2, 3 and 4 (Cabrera-Lafaurie *et al.,* 2012):

$$q=K_F C_e^{1/nf} \quad (2)$$

$$\frac{q}{q_m}=\frac{K_L C_e}{1+K_L C_e} \quad (3)$$

$$\frac{q}{q_m}=\frac{K_{LF} C_e^{1/n_{LF}}}{1+K_L C_e^{1/n_{LF}}} \quad (4)$$

Where; q represents the quantity adsorbed, q_m denotes the hights adsorption capacity, K_F, K_L and K_{LF} signify the interaction coefficients of Freundlich, Langmuir, and Langmuir-Freundlich, respectively, and the parameter n_F y n_{LF} are dimension constants that reflects the degree of heterogeneity of the adsorbent.

The pseudo-first-order kinetic model has been used to describe sorption kinetics, according to Eq. 5 (Wang *et al.,* 2021).

$$\log(q_e-q_t)=\log q_e-K_1/(2.303t) \quad (5)$$

Where; log (*qe-qt)* represents the logarithm of the equilibrium adsorption capacity. The parameter qt (mg/g) represents the amount adsorbed at a specific time t (min), while K_1 (per minute - /min) corresponds to the rate constant for the pseudo-first-order kinetic model.

The pseudo second (2nd) order kinetic model, which is based on equilibrium adsorption, using Eq. 6 (Wang *et al.,* 2021):

$$\frac{t}{q_t}=\frac{1}{K_2 q_e^2}+(1/q_e)t \quad (6)$$

Where; K_2 as gram per milligram per minute (g/mg/min) represents the rate constant of the pseudo-2nd -order equation. Tests were performed with wastewater for the small-scale application of the adsorbent employed. The samples were found to be contaminated with 100 ppm of Cd and Pb, and their concentration was determined. For this, 50 mg of adsorbent were blended with 10 mL of the sample. All adsorption experiments were carried out in triplicates.

RESULTS AND DISCUSSION

Material characterization

The obtained material, according to BET analysis, revealed a specific surface area of 2.1 square meter per gram (m^2/g), a mean pore diameter of 15.45 nm, and a pore volume of 7.9 cubic millimeters per gram (mm^3/g), indicating a mesoporous structure. As per the IUPAC classification, materials that have pore sizes ranging from 2 to 50 nm are categorized as mesoporous (Ren *et al.,* 2023). This characteristic is

especially advantageous for the adsorption of metal ions such as Pb and Cd, as it facilitates their diffusion into the internal structure and provides accessible active sites. In the charcoal samples, the moisture level was measured at 8.4%, the volatile material was found to be 71.23%, and the ash content stood at 4.89%. Furthermore, studies have shown that reduced moisture and ash content can boost the adsorption capacity of the adsorbent, thus enhancing the effectiveness of the activated carbon (Kim *et al.,* 2023). The values obtained for moisture, volatile matter, and ash are consistent with those reported by Fuentes *et al.* (2024) and Franco da Rocha *et al.* (2024), who described adsorbent materials with characteristics similar to those observed in this study. The FTIR spectra of samples C and CM are shown in Figs. 1 and 2, respectively. The infrared spectrum of C exhibits several characteristic bands. A broad and poorly defined band is observed between 3600 and 3000 /cm, corresponding to the stretching

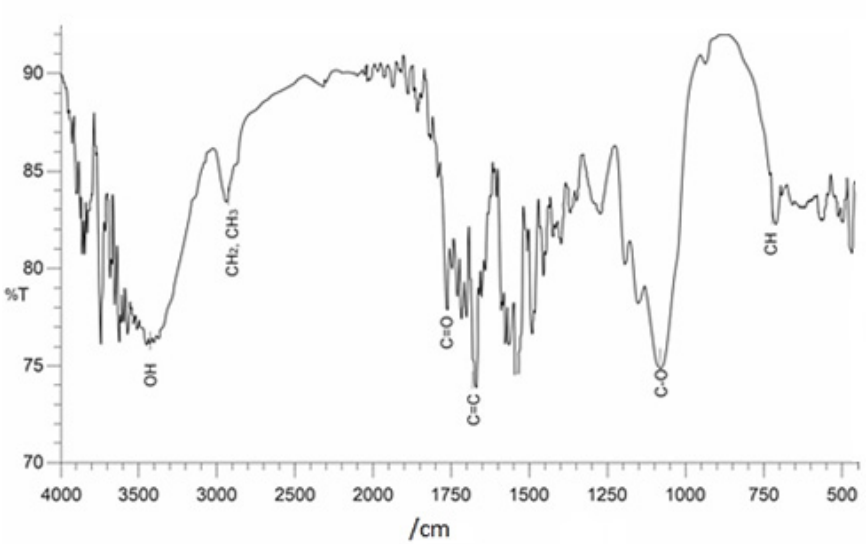

Fig. 1: FTIR spectra of C. %T is percentage transmittance

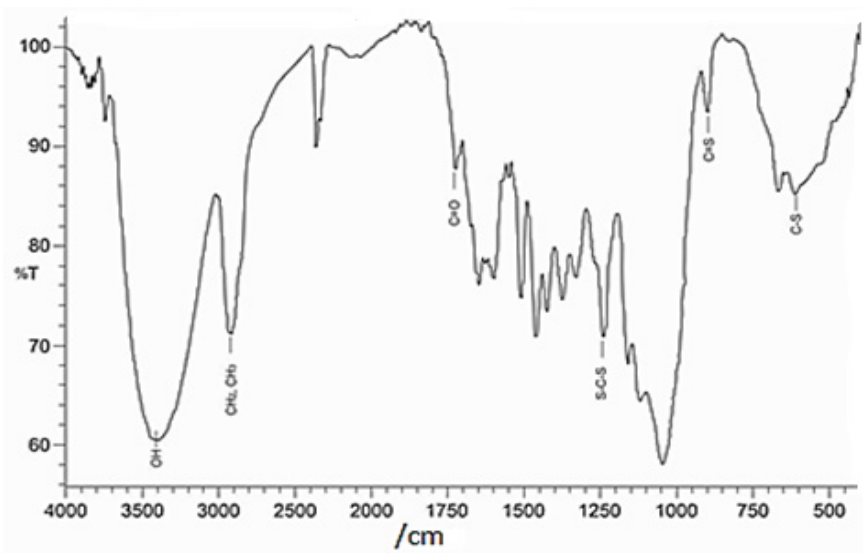

Fig. 2: FTIR spectra of CM

vibrations of oxygen (O) – hydrogen(H) groups. This implies that H bonds are present, probably related to remaining moisture or hydroxyl groups within the carbon structure. In the region between 3000 and 2800 /cm, signals are observed that are attributable to the stretching vibrations of methyl (CH_3) and methylene (CH_2) groups. The existence of these groups is often linked to carbonaceous compounds. Furthermore, bands appear at 1740 cm and 1620/cm, corresponding to the stretching vibrations of carbon C=O and C=C bonds, respectively. These results indicate the potential existence of carbonyl groups and double bonds in the carbon framework. The signals around 1400 and 1300/cm can be associated with the twisting and rocking vibrations of CH_3 and CH_2 groups. Finally, in the region near 1100 /cm, bands are observed that can be attributed to the stretching of C-O bonds, likely due to oxygenated compounds in the carbon. Meanwhile, the signals ranging from 800 and 600/cm are associated with the torsional vibrations of CH groups (He *et al*., 2017).

The infrared spectrum of the CM reveals supplementary traits that affirm the inclusion of xanthate groups. Signals in the region from 3000 to 2800 /cm, corresponding to the stretching vibrations of CH_2 and CH_3 groups, are still observable, albeit with lower intensity relative to the spectrum of unmodified C. New bands appear in the range of 1250–1000 /cm, which can be attributed to the stretching vibrations of C-O and sulfur (S) S-C-S bonds, characteristic of xanthate groups. The intense band at 1070 /cm is indicative of the presence of the C=S bond and C-S groups, confirming the functionalization of carbon with xanthate groups (Liang *et al.,* 2010). Furthermore, bands can be detected in the area ranging from 850 to 750 /cm, which further corroborates the existence of these groups. These findings affirm the successful enhancement of carbon through xanthates, leading to the introduction of new sulfur-containing functional groups and changes in the surface chemical composition of the material.

The UV-Vis spectroscopy results did not show the presence of xanthate group traces at any of the analyzed washing times. This indicates that the xanthate functionalization of the carbon is stable and that the material does not release detectable levels of these compounds into the aqueous solution under the experimental conditions employed. The lack of spectroscopic signals related to xanthates in the UV spectra implies that the employed synthesis and washing methods used are effective in eliminating any surplus reagent that is not attached to the surface of the material.

Effects of pH on Pb and Cd adsorption

Single-point adsorption experiments provide a straightforward and efficient method for gaining significant quantitative understanding of the influence of pH in heavy metal adsorption. pH is a key factor influencing the electrical state of the adsorbent surface, the level of ionic dissociation and the speciation of chemical species (Abou El-Reash, 2016; Zhu *et al.,* 2019). The influence of initial pH on the adsorption of Pb and Cd was examined across an initial pH spectrum ranging from 3.0 to 8.0. It is essential to emphasize that pH levels above 8 were excluded from this analysis, as they may cause the development of metal hydroxide precipitates, which would greatly obstruct the adsorption process and could lead to a misleading interpretation of adsorption (Nadarajah *et al.,* 2021). Fig. 3a-b presents the results obtained for adsorption on the adsorbents after 24 h of equilibrium at room temperature. A decrease in adsorption capacity at low pH levels is observed for both metals (Pb and Cd). This behavior was noted in both the C and CM. With the rise in pH of the solution, the adsorption capacity similarly increased, attaining a peak adsorption value at pH 6;this pattern was observed consistently for both adsorbents and metals. At this pH, the removal efficiencies reached 98% for Pb and 97% for Cd, indicating optimal adsorption conditions. The findings clearly demonstrate that pH levels have impacted the functional groups or surface charges of the adsorbent and the chemical speciation of the ions in the aqueous solutions. Furthermore, the effect of pH on adsorption capacity was evaluated through an analysis of variance (ANOVA), which showed significant differences for both metals, with an F-value of (5,12) surpassing 800 and a p-value < 0.001, confirming that pH has a crucial and statistically significant effect on removal efficiency.

The lower adsorption capacity at low pH is attributed to the increase in the concentration of hydronium ions (H_3O^+) as the pH of the solution decreases. This increase leads to competition between $H_3O^+$and metal cations for the active sites on the adsorbent, thereby affecting the adsorption capacity of Pb and Cd ions. This finding aligns with

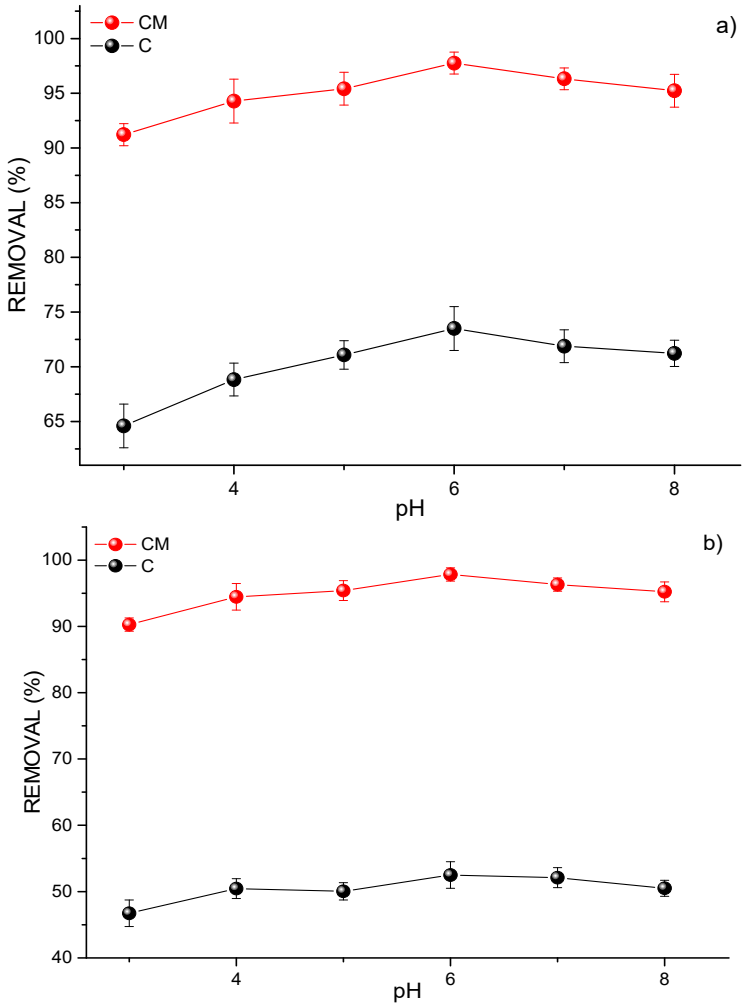

Fig. 3: Effect of solution pH on the adsorption of Pb (a) and Cd (b)

research that discusses the extraction of Pb^{2+} utilizing mesoporous activated carbons sourced from kenaf fiber through physical activation (Mandal *et al.,* 2021). Similar findings have been reported in other studies, where the adsorption of Pb^{2+} ions was highest at pH 6 in experiments conducted with activated carbons derived from apricot stone (Mouni *et al.,* 2021). Comparable findings were observed for different kinds of activated carbons at pH 6 (Purkait *et al.,* 2007). Likewise, comparable outcomes were obtained for the adsorption of Cd^{2+} on activated carbon derived from shrimp shell, with maximum removal % reported in the pH range of 6–7 (Guo *et al.,* 2021). This indicates that adsorption takes place more efficient at mildly acidic and neutral pH levels, contingent upon the characteristics of the adsorbent and the particular conditions involved. Speciation studies in aqueous solutions have shown that Pb and Cd ions remain predominantly in their Pb^{2+} and Cd^{2+} forms within the pH range of 5–6.5. At higher pH values, lead hydroxide $(Pb(OH)^{+})$ and cadmium hydroxide $(Cd(OH)^{+})$ emerge as new species (Pagnanelli *et al.,* 2003; Sheng *et al.,* 2004). These observations elucidate the reason behind the highest removal percentages for both chemical species occurring within this pH range. This behavior is also favored by the fact that, within the pH range of 5–6.5, the surface of the adsorbent becomes deprotonated

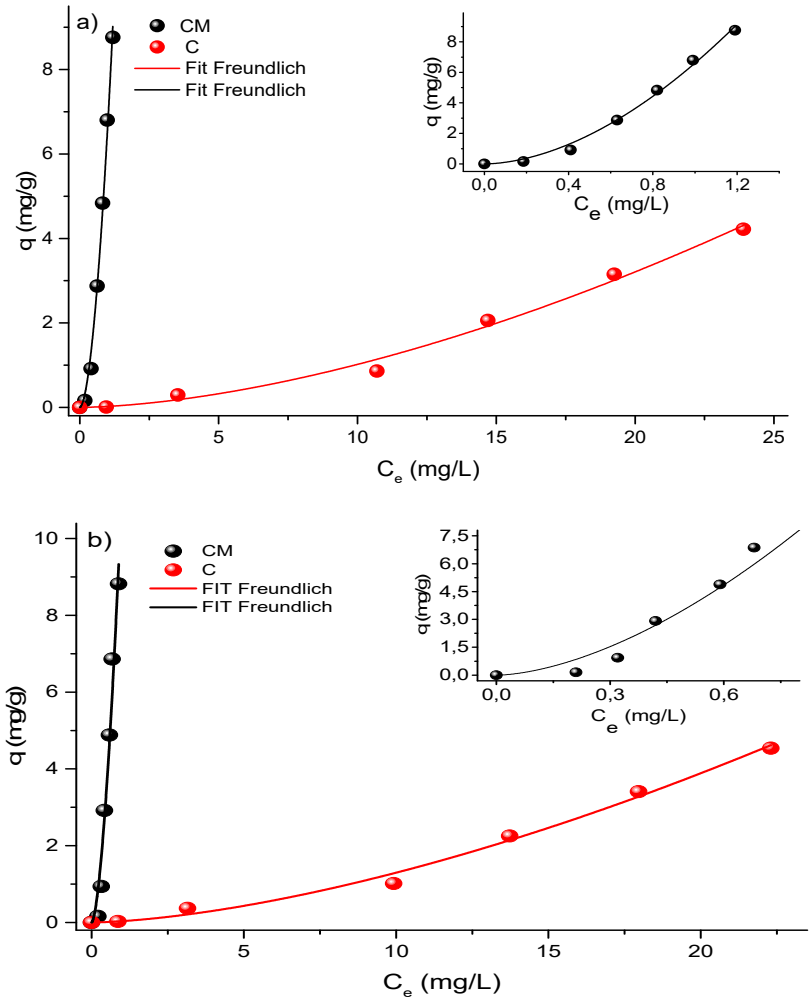

Fig. 4: Adsorption isotherms of Pb^{2+} (a) and Cd^{2+} (b) on C and CM.

and negatively charged. Consequently, a force of attraction is established between the negatively charged surface and the metal cations (Abbas *et al.,* 2016). When comparing the adsorption capacities of C and CM, as shown in Fig. 3, a significant improvement is observed in the removal properties of the modified adsorbent compared to the unmodified one. The adjusted resin exhibits a greater adsorption capacity throughout the complete range of pH levels assessed for both metals. This outcome is due to the chemical alteration of the surface by incorporating sulfur-containing groups, like xanthates, known for their strong attraction to heavy metals (Liang *et al.,* 2009).

Adsorption isotherms

Equilibrium isotherms are models that play a crucial role in explaining the interaction mechanism between the solute and the adsorbents. The adsorption process's efficiency is examined, offering insights into the affinity and attributes of the adsorbent. In general, the adsorption process depends on the pH of the solution, as evidenced by the results on the effect of pH on the adsorption capacities of metal ions. Thus, pH 6 was identified as the optimal condition for conducting equilibrium isotherm analyses. The equilibrium adsorption data for individual Pb and Cd ions are presented in Fig. 4a-b. It is important to note

Table 1: Adsorption isotherm parameters

Metal	Material	Lamgmuir-Freundlich					Freundlich			
		q_m (mg/g)	K_{FL}(L/mg)	n_{LF}	AIC	AICc	K_F(L/mg)	n_F	AIC	AICc
Pb^{+2}	C	6.820	0.0002	0.35	27.69	39.692	0.022	0.60	24.32	28.318
	CM	15.720	0.7799	0.36	46.19	54.192	6.606	0.56	21.50	24.496
Cd^{+2}	C	7.199	0.0002	0.34	30.14	38.141	0.034	0.63	29,50	32.501
	CM	11.535	4.81	0.30	20.91	28.913	11.32	0.60	9.70	12.698

that the adsorption capacities were considerably impacted by the changes implemented on the adsorbents (for instance, the addition of sulfur-containing groups), underscoring the efficiency of the process, which achieved an approximate 190% increase when to C. Studies have reported that sulfur-containing groups, particularly xanthates, exhibit high affinity for heavy metals and high stability constants for the metal complexes formed by these groups (Liang *et al.,* 2009; Panda *et al.,* 2008; Chakraborty *et al.,* 2006). Pb and Cd ions can be adsorbed onto the carbon resin via an ion exchange process, and/or complexation mechanisms. This is attributed to xanthate groups being classified as soft ligands based on the hard-soft acid-base (HSAB) concept, which exhibit a strong affinity for forming coordination complexes with divalent metals. According to HSAB principles, soft ligands have a strong affinity for soft acids such as Pb^{2+} and Cd^{2+}. These metals, categorized as borderline to soft Lewis acids, easily create stable coordination complexes with sulfur-containing groups (Wang *et al.,* 2016). This complexation is a chemisorption mechanism that entails the sharing of valence electrons from the lone pair on the sulfur atom and the empty orbitals of the metal ions.

Furthermore, the equilibrium adsorption capacity of the C and CM initially exhibited a significant increase with higher initial concentrations of metal ions. This occurrence can be linked to the increased driving forces generated by sharper concentration gradients when there are elevated initial metal ion concentrations. Three isotherm models (Freundlich, Langmuir, and Langmuir-Freundlich) were applied to evaluate the adsorption capacity, adsorption intensity, and to fit the experimental data of C and CM used for the removal of Pb^{2+} and Cd^{2+} ions from aqueous solutions. The results of the study are presented in Table 1. The Akaike Information Criterion (AIC) was employed to identify the adsorption isotherm model that best fits the experimental data. The AIC is a statistical tool that considers the number of parameters in the models being evaluated when ranking them, using Eq. 7 (Akpa and Unuabonah, 2011):

$$AIC = 2k - n_i\left[\ln\left(\frac{SSR}{n_i - k}\right)\right] \quad (2)$$

Where; the symbol k corresponds to the parameter count in the isotherm model, n_i refers to the amount of data points, and SSR is defined as the sum of "squared residuals. When the number of observations (*ni*) is small, the AIC should be corrected, using Eq. 8 (Akpa and Unuabonah, 2011):

$$AIC_c = AIC + \left[\frac{2k(k+1)}{n_i - k - 1}\right] \quad (8)$$

The adsorption isotherm model with the minimum *AICc* value was selected as the most appropriate to describe the experimental equilibrium data. Considering that the data corresponding to the Langmuir model yielded negative values, which lack physical significance, this model was excluded from the isotherm model analysis. In every case examined, the traditional Freundlich isotherm model was favored for representing the equilibrium data compared to other isotherm models that have three or comparable parameters. This aligns with findings from previous studies on the adsorption of heavy metals onto modified carbon-based materials (Mandal *et al.,* 2021; Liang *et al.,* 2009; Borji *et al.,* 2021). Furthermore, the heterogeneity factors presented in Table 1 showed a good correlation with non-homogeneous surfaces, as expected, given that the modified carbons contain both inorganic and organic fractions that may act as individual or simultaneous adsorption sites. This observed correlation validates that the altered carbon possesses a complex and uneven surface (heterogeneity), a trait that, based on the data, is linked

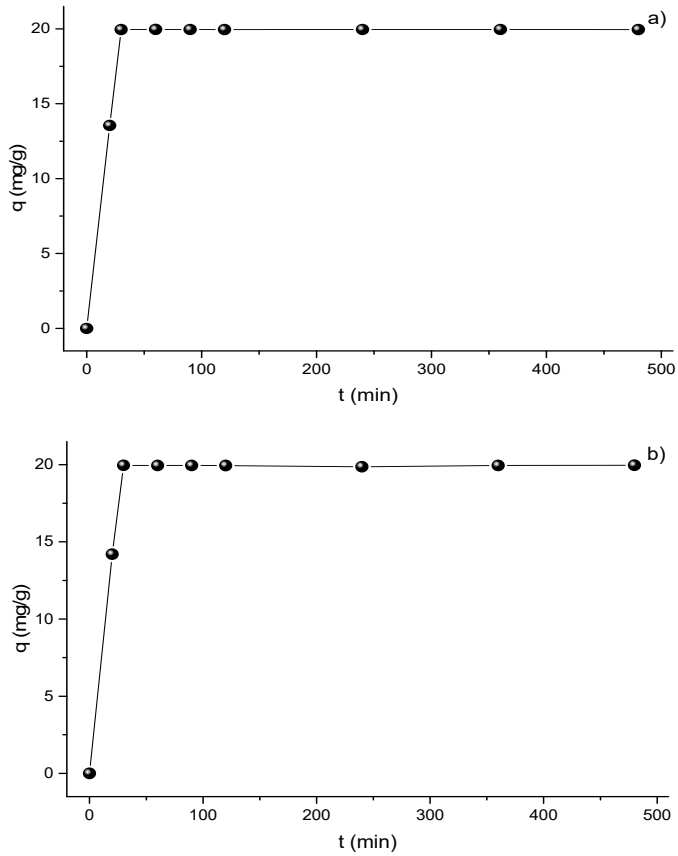

Fig. 5: Adsorption kinetics curve for Pb (a) and Cd (b)

to its structure and significantly impacts its capacity for heavy metal removal, influencing both the amount removed and the binding mechanisms. The results indicated that adsorption follows a Freundlich-type isotherm, characterizing the adsorption process as chemisorption. This is in agreement with the proposed adsorption mechanism, which entails a complexation process, leading to the formation of coordination complexes with Pb^{2+} and Cd^{2+}. Additionally, the Langmuir-Freundlich model is useful for defining the adsorption saturation point, as it includes the parameter q_m, which represents the maximum adsorption capacity of the material. This metric is vital for determining system constraints and potential effectiveness. According to the data presented in Table 1, the CM showed a q_m value of 15.720 mg/g for Pb and 11.535 mg/g for Cd, while the C exhibited significantly lower maximum capacities: 6.820 mg/g for Pb and 7.199 mg/g for Cd. The results demonstrate that the modified material exhibits a stronger attraction to metal ions, thus making it a superior alternative for the removal of metals from aqueous media.

Adsorption kinetics

Adsorption kinetics is significant as it helps to identify the rate at which metal ions are absorbed by the solid phase from aqueous solutions until equilibrium is attained. Furthermore, examining adsorption kinetics yields essential understanding of the adsorption mechanism, encompassing aspects invluding diffusion, surface reaction phenomena, and mass transfer. Adsorption kinetics were determined using solutions with a constant concentration of 100 ppm at pH 6, employing modified carbon while varying the contact time from 0.5 to 8 h. Two mathematical models were considered: the pseudo-first-order kinetic model and the pseudo-2nd-order kinetic model. From Fig. 5a-b,

Table 2: Adsorption kinetic parameters: Pseudo 2nd-order

Metal	qe (mg/g)	k_2 (/min)	$t_{1/2}=1/k_2qe$	R^2
Pb	20.00	0.020	0.1233	0.997
Cd	20.08	0.022	0.1118	0.996

it was noted that the adsorption process accelerates quickly within a brief time frame before reaching equilibrium. This behavior may be attributed to the progressive depletion of active sites on the CM as time progresses. Equilibrium was reached at 100 min, at which point the adsorbed concentration stabilized, with an adsorption capacity of 19.95 mg/g for Pb and 19.94 mg/g for Cd. Compared to other adsorbents used for the removal of heavy metals, the equilibrium time obtained in this study is competitive. Katariya *et al.* (2021) reported equilibrium times exceeding 120 min for the adsorption of Pb^{2+} and Cd^{2+} using a cationic ion-exchange resin modified with ethylenediaminetetraacetic acid (EDTA), while Wattanakornsiri *et al.* (2022) reported contact times close to 180 min using biosorbents derived from local fruit peels. The findings indicate that the xanthate-modified resin demonstrates effective adsorption kinetics, positioning it as a suitable option for the swift elimination of heavy metals in water-based environments. In addition to its rapid adsorption kinetics, the adsorption capacity of the xanthate-modified resin is comparable or superior to that of various materials reported in the literature. Mkilima *et al.* (2024) reported an adsorption capacity of 4.8 mg/g for Pb^{2+} using activated carbon derived from banana peel, while Mondal *et al.* (2024) documented 17.2 mg/g for Cd^{2+} in a biochar derived from macroalgae biomass. Additionally, Ofudje *et al.* (2015) reported an adsorption capacity of 22.1 mg/g for Pb^{2+} using alkali-modified coconut fruit as a biosorbent. These findings indicate the capability of the examined material for use in the remediation of contaminated water.

The pseudo-first-order kinetic model exhibited a correlation coefficient (R^2) close to zero, indicating a poor fit to the experimental data and suggesting that the adsorption process does not align with the assumptions of this kinetic model. Table 2 displays the rate constants for pseudo-2nd-order kinetic models concerning Pb and Cd, including the R^2 values. The agreement between the experimental data and the model predictions was assessed using R^2, which serve as a measure of how accurately the experimental data fit the kinetic models. A high R^2 value, close to 1, indicates that the model effectively describes the adsorption kinetics of metals.

The R^2 values derived from the linear regression analysis for both metal ions using the pseudo-first-order model were relatively low. Moreover, the equilibrium adsorption amounts, especially the discrepancy noted between the experimental adsorption capacity and the capacity estimated by the model, were significan. In contrast, the pseudo-2nd-order kinetic model yielded a much better fit, as indicated by higher correlation coefficients approaching unity (R^2 = 0.997). The graph illustrating t/qe in relation to t demonstrated a robust alignment between the experimentally derived values and the calculated values (Fig. 6a-b). Consequently, it can be inferred that the adsorption behavior of Pb and Cd ions onto CM adheres to the pseudo-2nd-order kinetic model. These findings are consistent with studies by Nadarajah *et al.* (2021), Liang *et al.* (2009), and Khalil *et al.* (2016), who examined the adsorption of Pb and Cd using modified carbon-based materials. These findings imply that the rate-controlling mechanism of the process is chemical adsorption or chemisorption, which depends on active sites instead of the concentration in the solution. This observation is consistent with the findings from adsorption isotherms and the proposed mechanism (complexation and ion exchange) (Yadav et al., 2013).

Laboratory-scale application

Studies focused on industrial wastewater aimed to analyze ion competition and the impact of natural organic matter (NOM) on the efficiency of metal ion removal in scenarios that more closely resemble real-world situations. Triplicate samples were taken, and the removal % of Pb and Cd were determined in water samples with an initial concentration (100 ppm) exceeding the permissible limit. This study was performed exclusively using the CM as this adsorbent demonstrated the highest efficiency for the removal of Pb and Cd compared to C. NOM

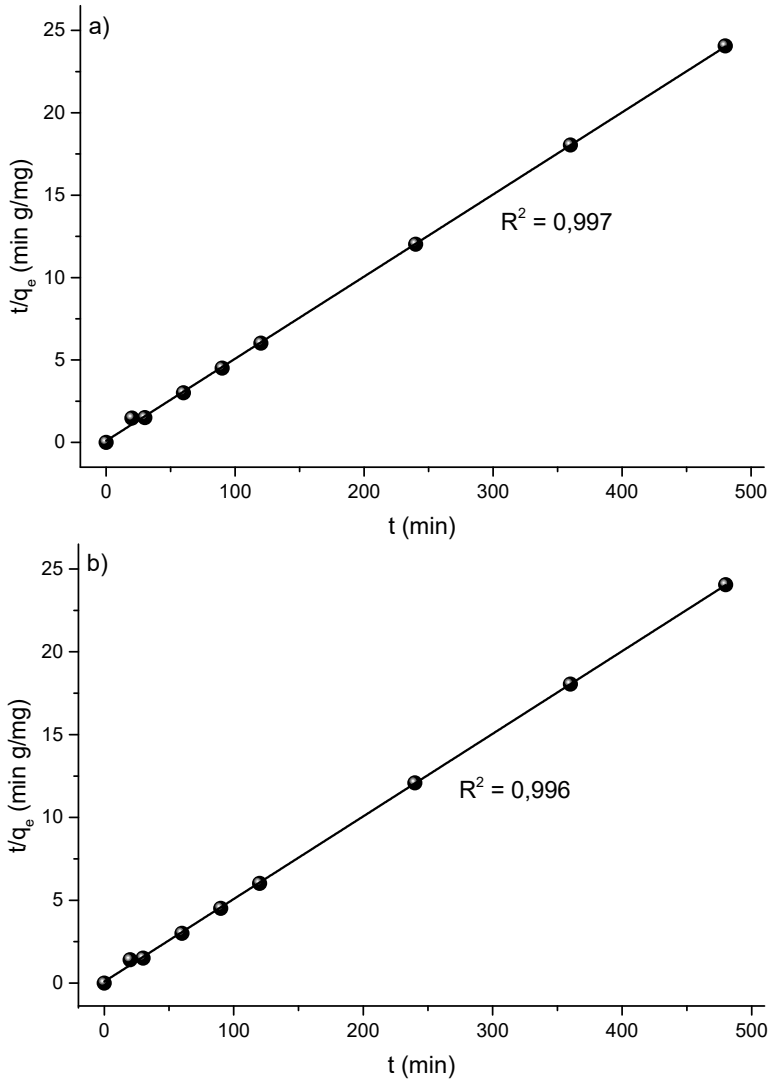

Fig. 6: Pseudo 2nd-order kinetics for the uptake of Pb (a) and Cd (b) on CM.

is well-known as a combination of polyfunctional organic acids, predominantly composed of humic and fulvic acids, which originate from the decomposition of organic materials from plants and animals. NOM is characterized as a complex mixture of organic acids and demonstrates significant reactivity with heavy metals (Jia *et al*., 2021). The interactions occurring between NOM and heavy metals can substantially can greatly alter the chemical behavior of these metals in environmental systems, influencing their mobility, availability to organisms, and potential toxicity (Zhou *et al.,* 2023). The characterization of this matrix revealed the presence of Fe (0.6 ppm), vanadium (V) (0.2 ppm), Cu (1 ppm), total nitrogen (21 ppm), total hardness (251 ppm as calcium carbonate-$CaCO_3$), chlorides (30 ppm), sulfates (14 ppm), NOM, and a pH of 7.2. The removal efficiency of Cd and Pb across five reuse cycles is depicted in Fig. 7. In the initial cycle (cycle 0), the CM achieves excellent removal efficiencies of 99.11% for Cd and 92% for Pb, demonstrating high performance in complex wastewater matrices. With the advancement of reuse cycles, there is a gradual decrease in the efficiency of removal for both metals. By cycle 4, Cd falls to about 93%, whereas the removal

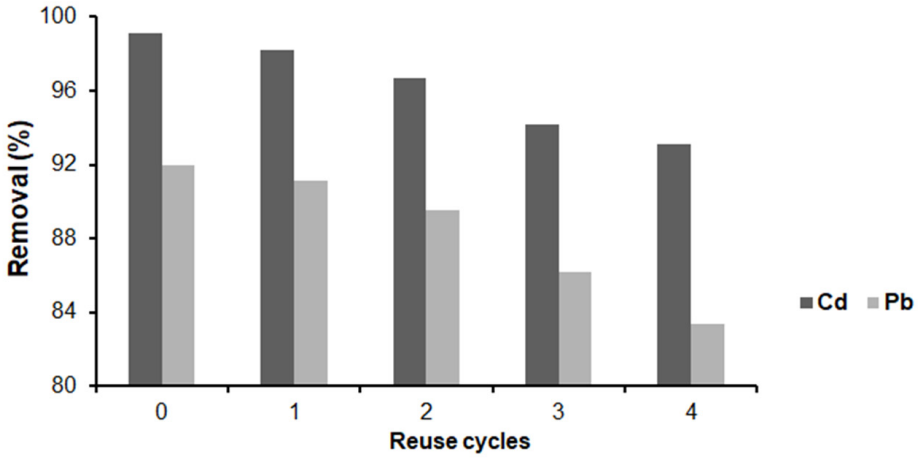

Fig. 7: % removal of heavy metals Pb and Cd in wastewater samples through reuse cycles.

of Pb declines sharply to roughly 83%, suggesting a more significant decrease in performance for Pb. This declining trend may be attributed to the saturation or partial deactivation of active sites on the CM surface, as well as potential structural changes in the material over repeated use. Furthermore, the competition for adsorption between metal ions and other substances present in the wastewater matrix could additionally obstruct removal efficiency during subsequent cycles. Despite this reduction, the material retains relatively high efficiency, particularly for Cd, suggesting strong and stable interactions between Cd^{2+} ions and the CM. As discussed in previous studies, NOM plays a crucial role in enhancing metal ion removal due to its diverse functional groups that facilitate ion exchange, chelation, and adsorption mechanisms (Tang *et al.*, 2014). Humic and fulvic acids, vital constituents of NOM, possess the ability to form stable complexes with heavy metals, which may also aid in the prolonged immobilization of Cd^{2+} and Pb^{2+} over multiple cycles (Du *et al.*, 2011; Wang *et al.*, 2017). Overall, while reuse cycles affect the efficiency, the CM still performs effectively, particularly in the removal of Cd, underscoring its potential for application in sustainable wastewater treatment systems. Additionally, the pH of the wastewater sample analyzed falls within the optimal range for the adsorption of both Cd^{2+} and Pb^{2+}, minimizing proton competition and the formation of less adsorbable metal hydroxide species. Overall, these results validate that ionic competition in actual wastewater did not impede the effectiveness of the adsorbent. On the contrary, the presence of NOM may have played a synergistic role, enhancing heavy metal uptake. These results reinforce the applicability of CM as a selective and effective adsorbent for treating industrial effluents contaminated with heavy metals.

Another comparative assessment of CM's performance relative to other adsorbents found in the literature (Table 3) emphasizes its considerable capability for heavy metal extraction. For Cd removal, the modified resin synthesized in this study demonstrated exceptional efficiency, reaching a removal rate of 99.11%. This surpasses the performance of several widely studied adsorbents, such as phosphate-modified sludge biochar (Zhou *et al.*, 2024), bioadsorbents derived from aged refuse (Manimekalai *et al.*, 2024), ion exchange resin (Marszałek *et al.*, 2023), a graphene oxide–silica composite (Mahmoudi *et al.*, 2020), and bamboo stem-derived biochar (Sable *et al.*, 2024). Significantly, it exceeded the performance of activated carbon made from banana peels (Mklima *et al.*, 2024). Its performance is comparable to that of carbon dots, as reported by Bhattacharjee *et al.* (2023). With respect to Pb removal, the enhanced resin accomplished a remarkable removal rate of 92.00%. Even though some materials exhibited somewhat greater efficiencies, such as sulfur-ferromagnetic nanoparticles (Song *et al.*, 2022), the resin still holds a competitive edge.

Table 3: Cd and Pb removal efficiencies of CM and other adsorbents

Adsorbent	Metal ions	Removal (%)	Sources
Banana peel-derived activated carbon (BPAC)	Pb Cd	92.40 89.90	Mkilima *et al*., 2024
Phosphate modified sludge biochar	Cd	97.00	Zhou, 2024
Activated carbons derived from plant-based materials	Pb Cd	> 90 > 90	Raji *et al*., 2023
Sulfur-ferromagnetic nanoparticles (SFMNs)	Pb	98.00	Song *et al*., 2022
Adsorbents derived from agricultural residues, such as treated rice and wheat husks	Pb Cd	95.00 92.00	Kwikima *et al*., 2021
Activated carbon obtained from pyrolysis of rice husks	Pb	95.36	Olupot *et al.,* 2024
Melanin-impregnated activated carbon	Pb	91.10	Manirethan and Balakrishnan, 2020
Ion exchange resin	Cd	95.50	Marszałek *et al*., 2023
Bioadsorbent (Aged refuse)	Cd	97.30	Manimekalai, and Subramanian, 2024
Bamboo stem derived biochar	Cd	90.60	Sable *et al*., 2024
Carbon dots	Cd	99.00	Bhattacharjee *et al*., 2023
Graphene oxide–silica composite	Cd	94.00	Mahmoudi *et al*., 2020
Cross-linked alginate-rice husk ash-graphene Oxide-chitosan	Pb	95.20	Nassar *et al*. (2025)
MOF-808-EDTA	Pb	92.00	Saeed *et al*., 2024
MOF: UiO-66-(SH)2	Pb	97.00	Abdollahi *et al*., 2020
Resin synthesized from modified mineral coal	Cd Pb	99.11 92.00	The present study

High removal rates have also been reported for adsorbents based on agricultural residues, including treated rice and wheat husks (Kwikima *et al*., 2021; Olupot *et al*., 2024), as well as for activated carbon produced via pyrolysis of rice husks (Raji *et al*., 2023), which generally achieved efficiencies above 90% for both metals under comparable conditions. The modified resin's performance is on par with or superior to other materials such as banana peel-derived activated carbon (Mklima *et al*., 2024), MOF-808-EDTA (Saeed *et al*., 2024), melanin-impregnated activated carbon (Manirethan and Balakrishnan, 2020), and the composite of cross-linked alginate, rice husk ash, graphene oxide, and chitosan (Nassar *et al*., 2025). Ultimately, the findings emphasize the exceptional capability of the modified resin in removing Cd and its competitive effectiveness in Pb removal. The sustainability of this material is not only reflected in its effectiveness but also in its production, as a key environmental benefit of the developed CM adsorbent lies in its origin. CM is synthesized from coal waste, a material that often presents disposal challenges. Utilizing this waste stream directly supports the principles of a circular economy by valorizing a by-product that would otherwise have limited economic reuse and could contribute to environmental problems through leaching of pollutants if not properly managed. This strategy minimizes the ecological strain related to standard waste management practices and could lower the demand for adsorbents derived from raw materials.

CONCLUSION

According to the outcomes of this study, the proximate and ultimate analyses demonstrated that the coal employed for resin production is classified as metallurgical and thermal, noted for its high volatility and carbon content, coupled with low levels of ash, moisture, and sulfur levels. These physicochemical properties enhance the adsorption capacity of the adsorbent. The adsorption performance of the CM for Pb and Cd ions significantly improved compared to C, achieving high removal percentages (98% for Pb and 97% for Cd). This improvement is due to the effective integration of sulfur-containing functional groups, especially xanthates, which promote complexation with divalent metal ions. The equilibrium adsorption data best fit the Freundlich isotherm, confirming the heterogeneous nature of the adsorbent surface and suggesting multilayer adsorption and strong metal-sorbent interactions. Moreover, kinetic studies

showed that the pseudo-2nd-order model provided the best fit ($R^2 = 0.997$), indicating that the rate-limiting step is likely chemisorption, involving valence forces through sharing or exchange of electrons. The CM demonstrated swift kinetics, achieving equilibrium within 100 minutes, exceeding the performance of various adsorbents noted in previous studies. The CM demonstrated remarkable performance even in complex matrices such as wastewater containing NOM, achieving 99.11% and 92% removal of Cd and Pb, respectively. This points to its possible use in real-life contexts, where interference from competing ions frequently occurs. The interaction of NOM with heavy metals likely enhanced adsorption efficiency through additional complexation pathways. This study's findings demonstrate that xanthate-modified coal can be an effective, cost-effective, and sustainable option for adsorbing contaminants from water. Future studies could further explore its regeneration capacity and long-term operational stability, which are essential parameters for scaling up this material in practical water treatment applications.

AUTHOR CONTRIBUTIONS

F. Fuentes Gandara, as the corresponding author, was responsible for analyzing the data and drafting the manuscript. W. Cabrera Lafaurie contributed significantly to the creation of tables and figures and took part in writing the manuscript. I. Piñeres Ariza was in charge of supervising the experimental work and performing a preliminary data evaluation. E. Espinosa – Fuentes participated in shaping the research proposal and provided a critical revision of the manuscript. J. Marrugo Negrete monitored specific phases of the experimental process and contributed to the interpretation of the data obtained. J. Pinedo Hernández contributed to research supervision, analysis of the results, and the preparation of the final manuscript.

ACKNOWLEDGEMENT

The authors are grateful to Universidad de la Costa and Universidad de Córdoba for providing the necessary facilities that enabled the experimental activities of this study.

CONFLICT OF INTEREST

The authors declare no potential conflict of interest regarding the publication of this work. In addition, the ethical issues including plagiarism, informed consent, misconduct, data fabrication and, or falsification, double publication and, or submission, and redundancy have been completely witnessed by the authors.

OPEN ACCESS

©2025 The author(s). This article is licensed under a Creative Commons Attribution 4.0 International License, which permits use, sharing, adaptation, distribution and reproduction in any medium or format, as long as you give appropriate credit to the original author(s) and the source, provide a link to the Creative Commons license, and indicate if changes were made. The images or other third-party material in this article are included in the article's Creative Commons license, unless indicated otherwise in a credit line to the material. If material is not included in the article's Creative Commons license and your intended use is not permitted by statutory regulation or exceeds the permitted use, you will need to obtain permission directly from the copyright holder. To view a copy of this license, visit: http://creativecommons.org/licenses/by/4.0/

PUBLISHER'S NOTE

GJESM Publisher remains neutral regarding jurisdictional claims about published maps and institutional affiliations.

Positive AI Statement

During the preparation of this work the author(s) have used Artificial Intelligence (exclusively for the translation into English of paragraphs originally written in Spanish). After using this tool/service, the authors reviewed and edited the content as needed and take full responsibility for the content of the publication.

(For this reason, the GPTZero detector will evaluate the manuscript utilizing Generative AI, ensuring a high detection rate. If the manuscript relies heavily on Generative AI and AI-assisted technologies, it will be archived without further options for appeal).

Negative AI Statement

The author(s) declare that no AI tools or services were not used or not highly applied during the preparation of this work.

ABBREVIATIONS

2nd	Second
%	Percent
%T	Percentage transmittance
°C	Degrees Celsius
/cm	Per centimeter
/min	Per minute
µm	Micrometer
AIC	The Akaike Information Criterion
Al	Aluminum
ANOVA	Analysis of Variance
ASTM	American Society for Testing Materials
AIM	Adsorption isotherm models
ASTM	American Society of Testing and Materials
BET	Brunauer, Emmett, and Teller
C	Unmodified mineral coal
Cd	Cadmium
$Cd(OH)^+$	Cadmium hydroxide
$Cd(NO_3)_2 \cdot 4H_2O$	Tetrahydrated cadmium nitrate
C_0	Initial concentration
$CaCO_3$	Calcium carbonate
Ce	Equilibrium concentration
CH_2	Methylene
CH_3	Methyl
CM	Modified mineral coal
cm	Centimeter
Cr	Chromium
CS_2	Carbon disulfide
Cu	Copper
DNA	Deoxyribonucleic acid
EDTA	Ethylenediaminetetraacetic acid
Fe	Iron
Fig.	Figure
FAOSTAC	Food and Agriculture Organization of the United Nations Statistical Database
FTIR	Fourier transform infrared spectroscopy
Fig.	Figure
g	Gram
g/mg/min	Gram per milligram per minute
h	Hour
H	Hydrogen
H_3O^+	Hydronium ions
HCl	Hydrochloric acid
Hg	Mercury
HNO_3	Nitric acid
HSAB	Hard Soft Acid Base
ICP-OES	Inductively coupled plasma optical emission spectrometer
k	Constant associated with the adsorption capacity of the adsorbent
k_1	Rate constant for pseudo-first-order kinetics
k_2	Rate constant for the pseudo second-order kinetic model
KBr	Potassium bromide
K_f	Interaction coefficients of Freundlich
K_l	Interaction coefficients of Langmuir
K_{LF}	Interaction coefficients of Langmuir-Freundlich
KOH	Potassium hydroxide
L	Liter
L/mg	Liter per milligram
ln(qe−qt)	Logarithm of the adsorbate amount not yet reached equilibrium (*qt*) at a specific time (*t*)
Log qe	Logarithm of the amount of adsorbate adsorbed at equilibrium per unit mass of adsorbent
M	Molarity
min	Minute
mg/L	Milligram per liter
mg/mL	Milligram per milliliter

mg/g	Milligram per gram
m^2/g	Square meter per gram
mm^3/g	Cubic millimeters per gram
$mg/g\ (L/g)^{1/n}$	Milligram per gram, multiplied by liter per gram raised to the inverse power of *n*
mL	Milliliter
mm	Millimeter
n	Constant related to the affinity (adsorption intensity) between the adsorbent and the solute
NaOH	Sodium hydroxide
n_F	Constant that reflects the degree of heterogeneity of the adsorbent of Freundlich
Ni	Nickel
n_{LF}	Constant that reflects the degree of heterogeneity of the adsorbent of Langmuir-Freundlich
n_i	Number of data points
nm	Nanometer
NOM	Natural Organic Matter
O	Oxygen
Pb	Lead
$Pb(OH)^+$	Lead hydroxide
$Pb(NO_3)_2$	Lead nitrate
pH	Potential of hydrogen
pKa	Acid dissociation constant
Ppm	Parts per million
q	Quantity absorbed
qe	Equilibrium adsorption capacity
q_m	Highest adsorption capacity
qt	Amount adsorbed at time t
R^2	Correlation coefficients
rpm	Revolutions per minute
S	Sulfur
SSR	Sum of squared residuals
t	Time
UNDP	United Nations Development Programme
UV-Vis	Ultraviolet visible
V	Volume of solution
W	Adsorbent mass

REFERENCES

Abbas, A.; Al-Amer, A.M.; Laoui, T.; Al-Marri, M.J.; Nasser, M.S.; Khraisheh, M.; Atieh, M.A., (2016). Heavy metal removal from aqueous solution by advanced carbon nanotubes: critical review of adsorption applications. Sep. Purif. Technol., 157: 141–161 **(21 pages)**.

Abdollahi, N.; Razavi, S.A.A.; Morsali, A.; Hu, M.L., (2020). High capacity Hg (II) and Pb (II) removal using MOF-based nanocomposite: cooperative effects of pore functionalization and surface-charge modulation. J. Hazard. Mater., 387: 121667 (**8 pages**).

Abou El-Reash, Y.G., (2016). Magnetic chitosan modified with cysteine-glutaraldehyde as adsorbent for removal of heavy metals from water, J. Environ. Chem. Eng., 4: 3835–3847 **(13 pages)**.

Akinterinwa, A.; Reuben, U.; Atiku, J.U.; Adamu, M., (2022). Focus on the removal of lead and cadmium ions from aqueous solutions using starch derivatives: A review. Carbohydr. Polym., 290: 119463 **(19 pages)**.

Akpa, O.M.; Unuabonah, E.I., (2011). Small-sample corrected Akaike information criterion: an appropriate statistical tool for ranking of adsorption isotherm models. Desalination. 272: 20–26 **(7 pages)**.

Arul, A.; Kavitha, S.; Christus, A.A.B.; Surya, V.J.; Ravikumar, A.; Sivalingam, Y., (2023). Enhanced removal of Pb (II) and Cd (II) ions from aqueous systems using coated magnetic nanoparticles in activated carbon derived from corncob waste. Surf. Interfaces. 40: 103095 **(19 pages)**.

Ben-Ali, S.; Jaouali, I.; Souissi-Najar, S.; Ouederni, A., (2017). Characterization and adsorption capacity of raw pomegranate peel biosorbent for copper removal. J. Cleaner Prod., 142: 3809-3821 (**13 pages**).

Benkő, M.; Puskás, S.; Király, Z., (2013). Application of mass spectrometry for study of the adsorption of multicomponent surfactant mixtures at the solid/solution interface. Adsorption. 19: 71-76 (**6 pages**).

Borji, H.; Ayoub, G.M.; Bilbeisi, R.; Nassar, N.; Malaeb, L., (2020). How effective are nanomaterials for the removal of heavy metals from water and wastewater? Water Air Soil Pollut. 231: 1–34 (**35 pages**).

Cabrera-Lafaurie, W.A.; Román, F.R.; Hernández-Maldonado, A.J., (2012). Transition metal modified and partially calcined inorganic–organic pillared clays for the adsorption of salicylic acid, clofibric acid, carbamazepine, and caffeine from water. J. Colloid Interface Sci., 386(1): 381-391 (**11 pages**).

Chakraborty, S.; Tare, V., (2006). Role of various parameters in synthesis of insoluble agro-based xanthates for removal of copper from wastewater. Bioresour. Technol., 97: 2407–2413 (**7 pages**).

Chakraborty, R.; Asthana, A.; Singh, A.K.; Jain, B.; Susan, A.B.H., (2022). Adsorption of heavy metal ions by various low-cost adsorbents: a review. Int. J. Environ. Anal. Chem., 102(2):

342-379 (**38 pages**).
Cheng, S.; Zhao, S.; Guo, H.; Xing, B.; Liu, Y.; Zhang, C.; Ma, M., (2022). High-efficiency removal of lead/cadmium from wastewater by MgO modified biochar derived from crofton weed. Bioresour. Technol., 343: 126081 (**8 pages**).
Du, Y.; Lian, F.; Zhu, L., (2011). Biosorption of divalent Pb, Cd and Zn on aragonite and calcite mollusk shells. Environ. Pollut., 159: 1763–1768 (**6 pages**).
El Mouden, A.; El Messaoudi, N.; El Guerraf, A.; Bouich, A.; Mehmeti, V.; Lacherai, A.; Jada, A.; Américo-Pinheiro, J.H.P., (2023). Removal of cadmium and lead ions from aqueous solutions by novel dolomite-quartz@ Fe_3O_4 nanocomposite fabricated as nanoadsorbent. Environ. Res., 225: 115606 (**13 pages**).
Fakhar, N.; Khan, S.A.; Siddiqi, W.A.; Khan, T.A., (2021). Ziziphus jujube waste-derived biomass as cost-effective adsorbent for the sequestration of Cd^{2+} from aqueous solution: isotherm and kinetics studies. Environ. Nanotechnol. Monit. Manage., 16: 100570 (**8 pages**).
Franco da Rocha, S.A.; Rocha, B.C.d.S.; Moraes, L.E.Z.d.; Villaça, J.M.P.; Scapin, D.; Santo, D.E.; Gonzalez, R.d.S.; Junior, O.V.; Peron, A.P., (2024). Evaluation and simulation of the adsorption capacity of octocrylene sunscreen on commercial carbon and biochar from spent coffee beans. Processes., 12: 1249 (**15 pages**).
Fontenele, R.S.; Hidalgo, P.; Gutz, I.G.; Pedrotti, J.J., (2007). Flow injection analysis of ethyl xanthate by in-line dialysis and UV spectrophotometric detection, Talanta. 72(3): 1017-1022 (**8 pages**).
Fuentes-Gandara, F.; Pinedo-Hernández, J.; Gutiérrez, E.; Marrugo-Negrete, J.; Díez, S., (2021). Heavy metal pollution and toxicity assessment in Mallorquin swamp: a natural protected heritage in the Caribbean Sea, Colombia. Mar. Pollut. Bull., 167: 112271 (**8 pages**).
Fuentes-Gandara, F.; Piñeres, I.E.; Zambrano, A.M.; Castellar, G.; Herrera, C. H.; Castro, S.; Peluffo, G.; Pinedo-Hernández, J., (2024). Removal of direct navy-blue dye from aqueous solutions using banana peles. Global J. Environ. Sci. Manage., 10(3): 1067 – 1084 (**18 pages**).
Gebretsadik, H.; Gebrekidan, A.; Demlie, L., (2020). Removal of heavy metals from aqueous solutions using *Eucalyptus camaldulensis*: an alternate low-cost adsorbent. Cogent Chem., 6(1): 1720892 (**17 pages**).
Gode, F.; Pehlivan, E., (2003). A comparative study of two chelating ion-exchange resins for the removal of chromium (III) from aqueous solution. J. Hazard. Mater., 100(1-3): 231-243 (**13 pages**).
Guo, J.; Song, Y.; Ji, X.; Ji, L.; Cai, L.; Wang, Y.; Zhang, H.; Song, W., (2019). Preparation and characterization of nanoporous activated carbon derived from prawn shell and its application for removal of heavy metal ions. Materials. 12: 241 (**17 pages**).
Gurnule, W.B.; Katkamwar, S.S., (2012). Selective removal of toxic metal ions from waste water using phenol formaldehyde type chelating resins. Rasayan J. Chem., 5(3): 365 – 375 (**11 pages**).
He, X.; Liu, X.; Nie, B.; Song, D., (2017). FTIR and Raman spectroscopy characterization of functional groups in various rank coals. Fuel., 206: 555-563 (**9 pages**).
Jasim, A.Q.; Ajjam, S.K., (2024). Removal of heavy metal ions from wastewater using ion exchange resin in a batch process with kinetic isotherm. S. Afr. J. Chem. Eng., 49: 43-54 (**12 pages**).
Jawad, A.H.; Malek, N.N.A.; Abdulhameed, A.S.; Razuan, R., (2020). Synthesis of magnetic chitosan-fly ash/ Fe3O4 composite for adsorption of reactive orange 16 dye: optimization by Box–Behnken design. J. Polym. Environ., 28(3): 1068-1082 (**15 pages**).
Jia, L.; Wu, W.; Zhang, J.; Wu, H., (2021). Insight into heavy metals (Cr and Pb) complexation by dissolved organic matters from biochar: impact of zero-valent iron. Sci. Total Environ., 793: 148469 (**9 pages**).
Kamaraj, M.; Kiruthika, N.; Saranya, T.; Aravind, J., (2025). Bibliometric analysis and impact of heavy metals contamination in soils. Global J. Environ. Sci. Manage., 11(1): 321-342 (**22 pages**).
Karim, M.R.; Aijaz, M.O.; Alharth, N.H.; Alharbi, H.F.; Al-Mubaddel, F.S.; Awual, M.R., (2019). Composite nanofibers membranes of poly (vinyl alcohol)/chitosan for selective lead (II) and cadmium (II) ions removal from wastewater. Ecotoxicol. Environ. Saf., 169: 479-486 (**8 pages**).
Katariya, S.N.; Kumar, S.; Yadav, R.B., (2021). Kinetics and thermodynamics of removal of metal ions using EDTA-modified cation ion exchange resin. Desal. Water Treat., 233: 133-149 (**17 pages**).
Khalil, T.E.; El-Dissouky, A.; Rizk, S., (2016). Equilibrium and kinetic studies on Pb^{2+}, Cd^{2+}, Cu^{2+} and Ni^{2+} adsorption from aqueous solution by resin 2,2'–(ethylenedithio) diethanol immobilized Amberlite XAD-16 (EDTDE-AXAD-16) with chlorosulphonic acid. J. Mol. Liq., 219: 533–546 (**14 pages**).
Khan, S.A.; Siddiqui, M.F.; Khan, T.A., (2020). Ultrasonic-assisted synthesis of polyacrylamide/bentonite hydrogel nanocomposite for the sequestration of lead and cadmium from aqueous phase: Equilibrium, kinetics and thermodynamic studies. Ultrason. Sonochem., 60: 104761 (**11 pages**).
Kim, S.; Lee, S.E.; Baek, S.H.; Choi, U.; Bae, H.J., (2023). Preparation of activated carbon from Korean anthracite: simultaneous control of ash reduction and pore development. Processes. 11(10), 2877 (**14 pages**).
Kumar, A.; Bhattacharya, T.; Vithanage, M., (2023). Valorization of waste biomass for biochar production and arsenic removal: a comparative assessment. Groundwater Sustainable Dev., 22: 100972 (**10 pages**).
Kwikima, M.M.; Mateso, S.; Chebude, Y., (2021). Potentials of agricultural wastes as the ultimate alternative adsorbent for cadmium removal from wastewater. A review. Sci. Afr., 13: e00934 (**14 pages**).
Li, S.; Li, S.; Wen, N.; Wei, D.; Zhang, Y., (2021). Highly effective removal of lead and cadmium ions from wastewater by bifunctional magnetic mesoporous silica. Sep. Purif. Technol., 265: 118341 (**11 pages**).https://doi.org/10.1016/j.

seppur.2021.118341

Liang, S.; Guo, X.; Feng, N.; Tian, Q., (2009). Application of orange peel xanthate for the adsorption of Pb^{2+} from aqueous solutions. J. Hazard. Mater., 170: 425–429 (**5 pages**).

Liang, S., Guo, X.Y.; Feng, N.C.; Tian, Q.H., (2010). Effective removal of heavy metals from aqueous solutions by orange peel xanthate. Trans. Nonferrous Met. Soc. China. 20: S187–S191 (**5 pages**).

Mahmoudi, E.; Azizkhani, S.; Mohammad, A.W.; Ng, L.Y.; Benamor, A.; Ang, W.L.; Ba-Abbad, M., (2020). Simultaneous removal of Congo red and cadmium (II) from aqueous solutions using graphene oxide–silica composite as a multifunctional adsorbent. J. Environ. Sci., 98: 151-160 (**10 pages**).

Mandal, S.; Calderon, J.; Marpu, S.B.; Omary, M.A.; Shi, S.Q., (2021). Mesoporous activated carbon as a green adsorbent for the removal of heavy metals and congo red: characterization, adsorption kinetics, and isotherm studies. J. Contam. Hydrol., 243: 103869 (**11 pages**).

Manimekalai, B.; Subramanian, S., (2024). Synthesized bioadsorbent using aged refuse for heavy metal removal in aqueous solution. Desalin. Water Treat., 320: 100862 (**11 pages**).

Manirethan, V.; Balakrishnan, R.M., (2020). Batch and continuous studies on the removal of heavy metals using biosynthesised melanin impregnated activated carbon. Environ. Technol. Innov., 20: 101085 (**18 pages**).

Marszałek, M.; Knapik, E.; Piotrowski, M.; Chruszcz-Lipska, K., (2023). Removal of cadmium from phosphoric acid in the presence of chloride ions using commercially available anion exchange resins. J. Ind. Eng. Chem., 118: 488–498 (**11 pages**).

Memon, S.Q.; Memon, N.; Shah, S.W.; Khuhawar, M.Y.; Bhanger, M.I., (2007). Sawdust—a green and economical sorbent for the removal of cadmium (II) ions. J. Hazard. Mater., 139(1): 116-121 (**6 pages**).

Mitra, S.; Chakraborty, A.J.; Tareq, A.M.; Emran, T.B.; Nainu, F.; Khusro, A.; Idris, A.M.; Khandaker, M.U.; Osman, H.; Alhumaydhi, F.A.; Simal-Gandara, J., (2022). Impact of heavy metals on the environment and human health: novel therapeutic insights to counter the toxicity. J. King Saud. Univ. Sci., 34(3): 101865 (**23 pages**).

Mkilima, T.; Zharkenov, Y.; Abduova, A.; Sarypbekova, N.; Kudaibergenov, N.; Sakanov, K.; Zhukenova, G.; Omarov, Z.; Sultanbekova, P.; Kenzhaliyeva, G., (2024). Utilization of banana peel-derived activated carbon for the removal of heavy metals from industrial wastewater. Case Stud. Chem. Environ. Eng., 10: 100791 (**10 pages**).

Mohammed, A.A.; Mahmood, H.S., (2013). Removal of Cu^{2+}, Pb^{2+}, and Ni^{2+} ions from simulated wastewater by ion exchange method on zeolite and purolite C105 resin. J. Eng., 19(10): 1327-1340 (**14 pages**).

Mondal, A.K.; Hinkley, C.; Kondaveeti, S.; Vo, P.H.N.; Ralph, P.; Kuzhiumparambil, U., (2024). Influence of pyrolysis time on removal of heavy metals using biochar derived from macroalgal biomass (*Oedogonium sp*). Bioresour. Technol., 414: 131562 (**13 pages**).

Mouni, L.; Merabet, D.; Bouzaza, A.; Belkhiri, L., (2011). Adsorption of Pb (II) from aqueous solutions using activated carbon developed from Apricot stone. Desalination. 276: 148–153 (**6 pages**).

Nadarajah, K.; Bandala, E.R.; Zhang, Z.; Mundree, S.; Goonetilleke, A., (2021). Removal of heavy metals from water using engineered hydrochar: kinetics and mechanistic approach. J. Water Process Eng., 40: 101929 (**12 pages**).

Nassar, A.A.; Mubarak, M.F.; El-Sawaf, A.K.; Zayed, M.A.; Hemdan, M., (2025). Efficient lead ion removal from aqueous solutions for wastewater treatment using a novel cross-linked alginate-rice husk ash-graphene oxide-chitosan nanocomposite. Int. J. Biol. Macromol., 284: 137983 (**13 pages**).

Olupot, P.W.; Wakatuntu, J.; Turyasingura, M.; Jjagwe, J.; Menya, E.; Okure, M., (2024). Optimization of heavy metal removal by activated carbon obtained as a co-product from fast pyrolysis of rice husks. Results Mater., 21: 100545 (**18 pages**).

Ofudje, E.A.; Akiode, O.K.; Oladipo, G.O.; Adedapo, A.E.; Adebayo, L.O.; Awotula, A.O., (2015). Application of raw and alkaline-modified coconut shaft as a biosorbent for Pb^{2+} removal. BioResources. 10: 3462-3480 (**19 pages**).

Pagnanelli, F.; Esposito, A.; Toro, L.; Veglio, F., (2003). Metal speciation and pH effect on Pb, Cu, Zn and Cd biosorption onto *Sphaerotilus natans*: Langmuir-type empirical model. Water Res., 37: 627–633 (**7 pages**).

Panda, G.C.; Das, S.K.; Guha, A.K., (2008). Biosorption of cadmium and nickel by functionalized husk of *Lathyrus sativus*. Colloids Surf. B., 62: 173–179 (**7 pages**).

Patel, H., (2020). Environmental valorisation of bagasse fly ash: a review. RSC Adv., 10(52): 31611-31621 (**11 pages**).

Pentari, D.; Vamvouka, D., (2019). Cadmium removal from aqueous solutions using nano-iron doped lignite. IOP Conference Series: Earth Environ. Sci., 221: 012135 (**8 pages**).

Pereira, I.C.; Carvalho, K.Q.; Passig, F.H.; Ferreira, R.C.; Rizzo-Domingues, R.C.P.; Hoppen, M.I.; Perretto, F., (2018). Thermal and thermal-acid treated sewage sludge for the removal of dye reactive red 120: characteristics, kinetics, isotherms, thermodynamics and response surface methodology design. J. Environ. Chem. Eng., 6(6): 7233-7246 (**14 pages**).

Požgajová, M.; Navrátilová, A.; Kovár, M., (2022). Curative potential of substances with bioactive properties to alleviate Cd toxicity: a review. Int. J. Environ. Res. Public Health., 19(19): 12380 (**42 pages**).

Purkait, M.K.; Maiti, A.; Dasgupta, S.; De, S., (2007). Removal of congo red using activated carbon and its regeneration. J. Hazard. Mater., 145: 287–295 (**9 pages**).

Raji, Z.; Karim, A.; Karam, A.; Khalloufi, S., (2023). Adsorption of heavy metals: mechanisms, kinetics, and applications of various adsorbents in wastewater remediation—a review. Waste. 1: 775–805 (**31 pages**).

Ren, Q.; Ma, Y.; Wei, F.; Qin, L.; Chen, H.; Liang, Z.; Wang, S., (2023). Preparation of Zr-MOFs for the adsorption of doxycycline hydrochloride from wastewater. Green Process. Synth., 12(1): 20228127 (**10 pages**).

Sabilillah, A.M.; Palupi, F.R.; Adji, B.K.; Nugroho, A.P., (2023). Health risk assessment and microplastic pollution in streams

through accumulation and interaction by heavy metals. Global J. Environ. Sci. Manage., 9(4): 719-740 (**22 pages**).

Sable, H.; Kumar, V.; Mishra, R.; Singh, V.; Roy, A.; Rai, A.K.; Ranjan, N.; Rustagi, S.; Pandit, S., (2024). Bamboo stem derived biochar for biosorption of cadmium (II) ions from contaminated wastewater. Environ. Nanotechnol. Monit. Manage., 21: 100936 (**8 pages**).

Saeed, F.; Reddy, K.A.; Sridhar, S., (2024). Efficient removal of environmentally hazardous heavy metal ions from water by NH2-MIL-101-Fe and MOF-808-EDTA based polyether sulfone adsorbents. Chem. Eng. J., 497: 154688 (**18 pages**).

Shang, Z.; Zhang, L.; Zhao, X.; Liu, S.; Li, D., (2019). Removal of Pb (II), Cd (II) and Hg (II) from aqueous solution by mercapto-modified coal gangue. J. Environ. Manage. 231: 391-396 (**6 pages**).

Sheng, P.X.; Ting, Y.P.; Chen, J.P.; Hong, L., (2004). Sorption of lead, copper, cadmium, zinc, and nickel by marine algal biomass: characterization of biosorptive capacity and investigation of mechanisms. J. Colloid Interface Sci., 275: 131–141 (**11 pages**).

Sireesha, S.; Agarwal, A.; Sopanrao, K.S.; Sreedhar, I.; Anitha, K.L., (2022). Modified coal fly ash as a low-cost, efficient, green, and stable adsorbent for heavy metal removal from aqueous solution. Biomass Convers. Biorefin., 1-23 (**23 pages**).

Song, H.; Kumar, A.; Zhang, Y., (2022). A novel approach for the removal of Pb^{+2} and Cd^{2+} from wastewater by sulfur-ferromagnetic nanoparticles (SFMNs). Chemosphere. 287: 132156 (8 pages).

Sulistyowati, L.; Nurhasanah, N.; Riani, E.; Cordova. M.R., (2023). Heavy metals concentration in the sediment of the aquatic environment caused by the leachate discharge from a landfill. Global J. Environ. Sci. Manage., 9(2): 323-336 (**14 pages**).

Sun, Y.; Song, X.; Ma, J.; Yu, H.; Liu, G.; Chen, F., (2022). Preparation and characterization of a novel amidoxime-modified polyacrylonitrile/fly ash composite adsorbent and its application to metal wastewater treatment. Int. J. Environ. Res. Public Health. 19(2): 856 (**13 pages**).

Tambaru, D.; Djahi, B.S.; Ndii, M.Z., (2018). The effects of hard water consumption on kidney function: insights from mathematical modelling. In: AIP conference proceedings. 1. AIP Publishing LLC: 020020 (**8 pages**).

Tamizharasan, S.; Muralidharan, R.; Abirami, N.; Leelavathi, H.; Siva, A.; Kumarasamy, A.; Arulmozhi, R., (2023). Biomass derived carbon blended ion-exchange resins for the removal of toxic metal ions from wastewater. Optik., 283: 170930 (**11 pages**).

Tang, W.W.; Zeng, G.M.; Gong, J.L.; Liang, J.; Xu, P.; Zhang, C.; Huang, B.B., (2014). Impact of humic/fulvic acid on the removal of heavy metals from aqueous solutions using nanomaterials: a review. Sci. Total Environ., 468: 1014-1027 (**11 pages**).

UNDP, (2024). La dependencia del país y de los territorios de los hidrocarburos y el carbón en Colombia y la necesidad de la diversificación de las exportaciones y de la producción ante la transición energética.

Virolainen, S.; Wesselborg, T.; Kaukinen, A.; Sainio, T., (2021). Removal of iron, aluminium, manganese and copper from leach solutions of lithium-ion battery waste using ion exchange. Hydrometallurgy. 202: 105602 (**9 pages**).

Wang, F.; Lu, X.; Li, X.Y., (2016). Selective removals of heavy metals (Pb^{2+}, Cu^{2+}, and Cd^{2+}) from wastewater by gelation with alginate for effective metal recovery. J. Hazard. Mater., 308: 75–83 (**9 pages**).

Wang, W.; Chen, M.; Guo, L.; Wang, W.X., (2017). Size partitioning and mixing behavior of trace metals and dissolved organic matter in a south China estuary. Sci. Total Environ., 603: 434–444 (**11 pages**).

Wang, P.; Liu, W.; Xu, H.; Liu, G., (2021). Adsorption of Pb (II) cation from aqueous solutions by acid modified low-rank coal: an experimental study and simulation. Water Sci. Technol. 84(12): 3726-3737 (**12 pages**).

Wang, Y.; Li, J.; Wei, X.; Zhou, Z.; An, L.; Zheng, S., (2024a). Construction of two protein-SmtA-based bio-microspheres as efficient 'collector'of heavy metal ions. Int. Biodeterior. Biodegrad., 189: 105768 (**10 pages**).

Wang, L.; Zhao, H.; Li, S.; Guo, B.; Huang, X.; Gao, P.; Ji, P., (2024b). Simultaneous removal of methylene blue and cadmium from aqueous solution by a novel sulfonated material: Characterization, mechanism and application. Environ. Chem. Eng., 12(1): 111706 (**11 pages**).

Wattanakornsiri, A.; Rattanawan, P.; Sanmueng, T.; Satchawan, S.; Jamnongkan, T.; Phuengphai, P., (2022). Local fruit peel biosorbents for lead (II) and cadmium (II) ion removal from waste aqueous solution: a kinetic and equilibrium study. S. Afr. J. Chem. Eng., 42: 306-317 (**12 pages**).

Wong, C.W.; Barford, J.P.; Chen, G.; McKay, G., (2014). Kinetics and equilibrium studies for the removal of cadmium ions by ion exchange resin. J. Environ. Chem. Eng., 2(1): 698-707 (**10 pages**).

Yadav, S.K.; Singh, D.K.; Sinha, S., (2013). Adsorption study of lead (II) onto xanthated date palm trunk: kinetics, isotherm and mechanism. Desalin. Water Treat., 51(34-36): 6798-6807 (**10 pages**).

Yang, Y.; Wang, L.; Zhao, H.; Yan, F.; Li, S.; Guo, B.; Luo, C.; Huang, X.; Ji, P., (2023). Utilization of KOH-modified fly ash for elimination from aqueous solutions of potentially toxic metal ions. Environ. Res., 223: 115396 (**10 pages**).

Yuliani, G.; Qi, Y.; Hoadley, A.F.; Chaffee, A.L.; Garnier, G., (2012). Lignite clean up of magnesium bisulphite pulp mill effluent as a proxy for aqueous discharge from a ligno-cellulosic biorefinery. Biomass Bioenergy. 36: 411-418 (**8 pages**).

Zhou, Z.; Zhang, C.; Xi, M.; Ma, H.; Jia, H., (2023). Multi-scale modeling of natural organic matter–heavy metal cations interactions: aggregation and stabilization mechanisms. Water Res., 238, 120007 (**12 pages**).

Zhou, L., (2024). Improving the removal performance of cadmium from wastewater by phosphate modified sludge biochar: a mineral dissolution-precipitation perspective. Desalination Water Treat., 320: 100865 (**11 pages**).

Zhu, Y.; Fan, W.; Zhou, T.; Li, X., (2019). Removal of chelated heavy metals from aqueous solution: a review of current methods and mechanisms. Sci. Total Environ., 678: 253–266 (**14 pages**).

AUTHOR (S) BIOSKETCHES

Fuentes-Gandara, F., Ph.D., Professor, Department of Natural and Exact Sciences, Universidad de la Costa, Barranquilla, Colombia.
- Email: *fabioar20@hotmail.com*
- ORCID: 0000-0002-0681-0544
- Web of Science ResearcherID: GXV-7697-2022
- Scopus Author ID: 57192062455
- Homepage: https://www.researchgate.net/profile/Fabio-Fuentes

Cabrera-Lafaurie, W., Ph.D., Professor, Corporación Universitaria de Ciencias Empresariales, Educación y Salud – Corsalud, Barranquilla, Colombia.
- Email: *wilman.cabrera@unicorsalud.edu.co*
- ORCID: 0000-0002-9041-7576
- Web of Science ResearcherID: CIM-7743-2022
- Scopus Author ID: 37009535700
- Homepage: https://www.researchgate.net/profile/Wilman-Cabrera

Piñeres-Ariza, I., Ph.D., Professor, Department of Physics, Faculty of Basic Sciences, Universidad del Atlántico, Barranquilla, Colombia.
- Email: *ismaelpineres@mail.uniatlantico.edu.co*
- ORCID: 0000-0003-4871-6211
- Web of Science ResearcherID: GQB-0840-2022
- Scopus Author ID: 56017822200
- Homepage: https://www.researchgate.net/profile/Ismael-Pineres

Espinosa-Fuentes, E., Ph.D., Professor, Faculty of Engineering, Universidad Libre, Barranquilla, Colombia.
- Email: *eduardo.espinosaf@unilibre.edu.co*
- ORCID: 0000-0003-1653-5408
- Web of Science ResearcherID: DVL-0558-2022
- Scopus Author ID: 24340657400
- Homepage: https://www.researchgate.net/profile/Eduardo_Espinosa

Marrugo-Negrete, J., Ph.D. Professor, Faculty of Basic Sciences, Department of Chemistry, Universidad de Córdoba, Montería, Colombia.
- Email: *jmarrugo@correo.unicordoba.edu.co*
- ORCID: 0000-0002-3181-7529
- Web of Science ResearcherID: FJD-6078-2022
- Scopus Author ID: 23480310100
- Homepage: https://www.researchgate.net/profile/Jose-Marrugo-Negrete

Pinedo-Hernández, J., M.Sc., Assistant Professor, Faculty of Basic Sciences, Department of Chemistry, Universidad de Córdoba, Montería, Colombia.
- Email: *josejph@hotmail.com*
- ORCID: 0000-0002-4288-1788
- Web of Science ResearcherID: AAV-2548-2021
- Scopus Author ID: 55780076200
- Homepage: https://www.researchgate.net/profile/Jose-Pinedo-2

HOW TO CITE THIS ARTICLE

Fuentes-Gandara, F.; Cabrera-Lafaurie, W.; Piñeres-Ariza, I.; Espinosa-Fuentes, E.; Marrugo-Negrete, J.; Pinedo-Hernández, J., (2025). Removal of cadmium and lead using a sub-bituminous coal resin modified with xanthate groups. Global J. Environ. Sci. Manage., 11(3): 1035-1056.

DOI: 10.22034/gjesm.2025.03.10

URL: https://www.gjesm.net/article_724627.html